

Value-based Search in Execution Space for Mapping Instructions to Programs

Dor Muhlgay¹ Jonathan Herzig¹ Jonathan Berant^{1,2}

¹School of Computer Science, Tel-Aviv University

²Allen Institute for Artificial Intelligence

{dormuhlg@mail, jonathan.herzig@cs, joberant@cs}.tau.ac.il

Abstract

Training models to map natural language instructions to programs given target world supervision only requires searching for good programs at training time. Search is commonly done using beam search in the space of partial programs or program trees, but as the length of the instructions grows finding a good program becomes difficult. In this work, we propose a search algorithm that uses the target world state, known at training time, to train a *critic* network that predicts the expected reward of every search state. We then score search states on the beam by interpolating their expected reward with the likelihood of programs represented by the search state. Moreover, we search not in the space of programs but in a more compressed state of program executions, augmented with recent entities and actions. On the SCONE dataset, we show that our algorithm dramatically improves performance on all three domains compared to standard beam search and other baselines.

1 Introduction

Training models that can understand natural language instructions and execute them in a real-world environment is of paramount importance for communicating with virtual assistants and robots, and therefore has attracted considerable attention (Branavan et al., 2009; Vogel and Jurafsky, 2010; Chen and Mooney, 2011). A prominent approach is to cast the problem as semantic parsing, where instructions are mapped to a high-level programming language (Artzi and Zettlemoyer, 2013; Long et al., 2016; Guu et al., 2017). Because annotating programs at scale is impractical, it is desirable to train a model from instructions, an initial world state, and a target world state only, letting the program itself be a latent variable.

Learning from such weak supervision results in a difficult search problem at training time. The

model must search for a program that when executed leads to the correct target state. Early work employed lexicons and grammars to constrain the search space (Clarke et al., 2010; Liang et al., 2011; Krishnamurthy and Mitchell, 2012; Berant et al., 2013; Artzi and Zettlemoyer, 2013), but recent success of sequence-to-sequence models (Sutskever et al., 2014) shifted most of the burden to learning. Search is often performed simply using beam search, where program tokens are emitted from left-to-right, or program trees are generated top-down (Cheng et al., 2017) or bottom-up (Liang et al., 2017). Nevertheless, when instructions are long and complex and reward is sparse, the model may never find enough correct programs, and training will fail.

In this paper, we propose a beam-search algorithm for mapping a sequence of natural language instructions to a program. First, we capitalize on the target world state being available at training time and train a *critic* network that given the language instructions, current world state, and target world state estimates the expected future reward for each search state. In contrast to traditional beam search where states representing partial programs are scored based on their likelihood only, we also consider expected future reward, leading to a more targeted search at training time. Second, rather than search in the space of programs, we search in a more compressed execution space, where each state is defined by the result of executing a partial program, while tracking recent entities and actions. This makes the search space smaller, while allowing us to handle references to past entities and actions.

We evaluate on the SCONE dataset, which includes three different domains where long sequences of 5 instructions are mapped to programs. We show that while standard beam search gets stuck in a local optimum and is unable to discover

good programs for many examples, our model is able to bootstrap in this challenging setup, improving final performance by more than 25 points on average. We also perform extensive analysis and show that both value-based search as well as searching in execution space contribute to the final performance.

2 Background

Mapping instructions to programs invariably involves a *context*, such as a database or a robotic environment, in which the program (or logical form) is executed. The goal is to train a model given a training set $\{(x_{(j)} = (c_{(j)}, \mathbf{u}_{(j)}), y_{(j)})\}_{j=1}^N$, where c is the context, \mathbf{u} is a sequence of natural language instructions, and y is the target state of the environment after following the instructions, which we refer to as *denotation*. The model is trained to map the instructions \mathbf{u} to a program \mathbf{z} such that executing \mathbf{z} in the context c results in the denotation y , which we denote by $\llbracket \mathbf{z} \rrbracket_c = y$. Thus, the program \mathbf{z} is a latent variable we must search for at both training time and test time. When the sequence of instructions is long, search becomes hard, particularly in the early stages of training.

Recent work tackled the training problem using variants of reinforcement learning (RL) (Suhr and Artzi, 2018; Liang et al., 2018) or maximum marginal likelihood (MML) (Guu et al., 2017; Goldman et al., 2018). We now briefly describe MML training, which we based our training procedure on, and outperformed RL in past work under comparable conditions (Guu et al., 2017).

We denote by $\pi_\theta(\cdot)$ a model, parameterized by θ , that generates the program \mathbf{z} token by token from left to right. The model π_θ receives the context c , instructions \mathbf{u} and previously predicted program tokens $z_{1..t-1}$, and returns a distribution over the next program token z_t . The probability of a program prefix is defined to be: $p_\theta(z_{1..t} | \mathbf{u}, c) = \prod_{i=1}^t \pi_\theta(z_i | \mathbf{u}, c, z_{1..i-1})$. The model is trained using stochastic gradient descent to maximize the MML objective:

$$J_{MML} = \log \prod_{(x,y)} p_\theta(y | x) = \sum_{(c,\mathbf{u},y)} \log \sum_{\mathbf{z}} p_\theta(\mathbf{z} | \mathbf{u}, c) \cdot R(\mathbf{z}),$$

where $R(\mathbf{z}) = 1$ if $\llbracket \mathbf{z} \rrbracket_c = y$, and 0 otherwise (For brevity, we omit c and y from $R(\cdot)$).

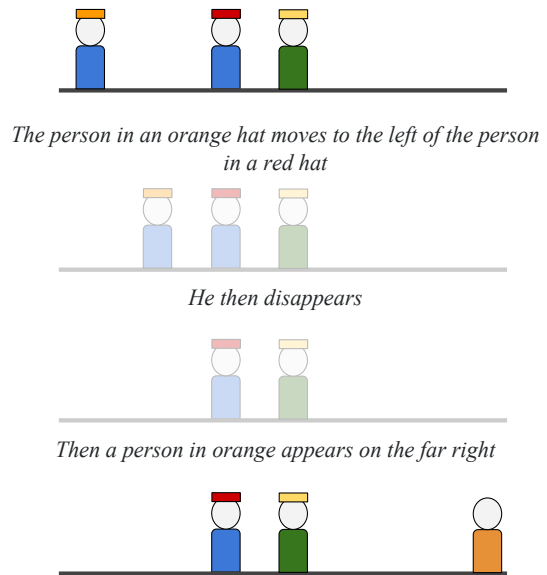


Figure 1: Example from the SCENE domain in SCONE (3 utterances), where people with different hats and shirts are located in different positions. Each example contains an initial world (top), a sequence of natural language instructions, and a target world (bottom). Intermediate world states and the program are latent.

The search problem arises because it is impossible to exhaustively enumerate the countable set of all programs, and thus the sum over programs is approximated by a small set of high probability programs (introducing some bias). Search is commonly done with *beam-search*, an iterative algorithm that builds an approximation of the highest probability programs according to the model. At each time step t , the algorithm constructs a beam B_t of at most K program prefixes of length t . Given a beam B_{t-1} , B_t is constructed by selecting the K most likely *continuations* of prefixes in B_{t-1} , according to $p_\theta(z_t | \cdot)$. The algorithm runs for a fixed number of iteration L , and returns all the complete programs that were discovered.

In this paper, our focus is the search problem that arises at training time when training from denotations, namely, we must find programs that execute to the right denotation. Thus, we would like to focus on scenarios where programs are long, and consequently vanilla beam search fails as a search algorithm. We next describe the SCONE dataset, which provides such an opportunity.

The SCONE dataset Long et al. (2016) presented the SCONE dataset, where a sequence of instructions needs to be mapped to a program consisting of a sequence of commands executed in an environment. The dataset comprises three do-

mains, where each domain includes several objects (such as *people* or *beakers*), each with different properties (such as *shirt color* or *chemical color*). SCONE provides a good environment for stress-testing search algorithms because a sequence of instructions needs to be mapped to a sequence of commands that result in the correct denotation. Figure 1 shows an example input from the SCENE domain.

Formally, the context in SCONE is a *world* that is specified by a list of positions, where each position may contain an object with certain properties. A formal language is defined to interact and manipulate the world. The formal language contains *constants* (e.g., numbers and colors), *functions* that allow to query the world and refer to various objects and intermediate computations, and *actions*, which are functions that modify the world state. Each command is composed of a single action and several arguments constructed recursively from constants and functions. For example, the command `MOVE(HASHAT(YELLOW), LEFTOF(HASSHIRT(BLUE)))`, contains the action `MOVE`, which moves a person to a specified position. The person is computed by `HASHAT(YELLOW)`, which queries the world for the position of the person with a yellow hat, and the target position is computed by `LEFTOF(HASSHIRT(BLUE))`, which queries the world for the position to the left of the person with a blue shirt. We refer to Guu et al. (2017) for a full description of the formal language.

Our goal is to train a model that given an initial world w^0 and a sequence of natural language utterances $\mathbf{u} = (u^1, \dots, u^M)$, will map each utterance u^i to a command z^i such that applying the program $\mathbf{z} = (z^1, \dots, z^M)$ on w^0 will result in the target world, i.e., $\llbracket \mathbf{z} \rrbracket_{w^0} = w^M = y$.

3 Markov Decision Process Formulation

To present our search algorithm, we first formulate the problem as a Markov Decision Process (MDP). We show in Section 4 that the graph induced by an MDP when searching in the space of programs is a tree. Conversely, our algorithm will search in a more compact execution space, where the MDP corresponds to a graph.

We represent the MDP as a tuple $(\mathcal{S}, \mathcal{A}, R, \delta)$, where \mathcal{S} is the state space, \mathcal{A} is the action space, $R(\cdot)$ is the reward function, and $\delta(\cdot)$ is a deterministic transition function. To define \mathcal{S} , we first

assume all program prefixes are executable, which can be easily done as we show below. The *execution result* of a prefix \tilde{z} in the context c , denoted by $\llbracket \tilde{z} \rrbracket_c^{ex}$, contains its denotation, but also additional information stored in the internal state of the executor, as we elaborate below. Let \mathcal{Z}_{pre} be the set of all valid programs prefixes. The set of states is defined to be $\mathcal{S} = \{(x, \llbracket \tilde{z} \rrbracket_c^{ex}) \mid \tilde{z} \in \mathcal{Z}_{pre}\}$, i.e., the input paired with the result of executing all possible program prefixes. Because many program prefixes have the same execution result, the *execution space* \mathcal{S} is much smaller than the space of programs.

The action set \mathcal{A} includes all possible program tokens,¹ and the transition function $\delta : \mathcal{S} \times \mathcal{A} \rightarrow \mathcal{S}$ is computed by the environment executor. Last, the reward $R(s, a) = 1$ iff the action a ends the program and leads to a state $\delta(s, a)$ where the denotation is equal to the target world y . The model $\pi_\theta(\cdot)$ is as a parameterized neural policy over the MDP that provides a distribution over the program vocabulary at each time step (details in Appendix A). Next, we precisely define the execution result $\llbracket \mathbf{z} \rrbracket_c^{ex}$.

Execution result We assume every program prefix can be executed, which can be done by writing programs in postfix notation, as described by Guu et al. (2017). For example, the instruction `MOVE(HASHAT(YELLOW), LEFTOF(HASSHIRT(BLUE)))` is written as `YELLOW HASHAT BLUE HASSHIRT LEFTOF MOVE`. With this notation, a partial program can be executed left-to-right by maintaining a *program stack*, ψ . At each time step, the executor pushes predicted constants (`YELLOW`) to ψ , and applies functions (`HASHAT`) by popping their arguments from ψ and pushing the computed result. Actions (`MOVE`) are applied by popping arguments from ψ and performing the action in the current world.²

Because the input is a *sequence* of utterances, each mapping to a command, whenever an action is predicted, the model moves to processing the next utterance, (and the stack ψ is emptied), until all utterances have been processed. To handle references to previous utterances, we must track previous actions and arguments, and so the executor maintains an *execution history*,

¹Decoding is grammar-constrained at training and test time to output syntactically valid program tokens only.

²Left-to-right decoding is equivalent to bottom-up decoding of the program tree in this case.

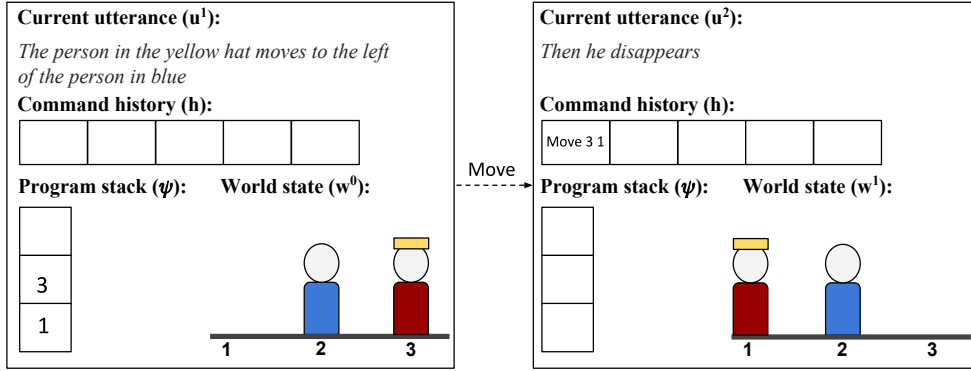


Figure 2: An illustration of a state transition in SCONE. The policy predicted the action token MOVE. Before the transition (left) the command history is empty, and the program stack contains the arguments 3 and 1 which were computed in previous steps. Note that the state does not include the partial program that computed those arguments. After transition (right) the executor popped the arguments from the program stack and applied the action MOVE 3 1: the man with the yellow hat moved to position 1 and the action is added to the execution history with its arguments. Since this action terminated the current command, the policy advances to the next utterance.

$\mathbf{h}^i = (e^1, \dots, e^i)$, which is a list of previously executed actions and their arguments (the formal language provides functions to query \mathbf{h}^i). Thus, the execution result of a program prefix is $\llbracket \tilde{z} \rrbracket_{w^0}^{ex} = (u_i, w^{i-1}, \psi, \mathbf{h}^{i-1})$, which includes the current utterance, current denotation, the program stack and the execution history.

Figure 2 illustrates an example transition from one state to another in the SCENE domain. Importantly, the state does not store the full program generated (only the execution history), and thus many different programs lead to the same state. Next, we describe a search algorithm in the state space of this MDP.

4 Searching in Execution Space

Model improvement relies on generating correct programs given a possibly weak model. Standard beam-search explores the space of all program token sequences up to some fixed length. We propose two technical contributions to improve search: (a) We simplify the search problem by searching for correct executions rather than correct programs (b) We use the target denotation at training time to better estimate partial program scores in the search space. We describe those next.

4.1 Execution space

Our task can be represented as a search problem in a graph. The space of programs can be formalized as a directed tree $T = (\mathcal{V}_T, \mathcal{E}_T)$, where vertices \mathcal{V}_T represent all program prefixes, and labeled edges \mathcal{E}_T represent all prefix continuations: an edge $e = (s_1 = z_{1..t-1}, s_2 = z_{1..t-1} \circ z_t)$, rep-

resents a continuation of the prefix $z_{1..t-1}$ with the token z_t , where \circ denotes concatenation. The root of the graph represents the empty sequence. Similarly, *Execution space* is a directed graph $G = (\mathcal{V}_G, \mathcal{E}_G)$ induced from the MDP described in Section 3. Graph vertices \mathcal{V}_G represent MDP states, which express execution results, and labeled edges \mathcal{E}_G represent transitions. An edge (s_1, s_2) labeled by program token z_t means that $\delta(s_1, z_t) = s_2$. Since multiple programs have the same execution result, execution space is a compressed representation of program space: multiple vertices in program space map to a single vertex in execution space. Figure 3 illustrates a set of programs in both program space and execution space.

Each path in execution space represents a different program prefix, and the path’s final state represents its execution result. Program search can therefore be reduced to execution search: given an example (c, \mathbf{u}, y) and a model π_θ , we can use π_θ to explore in execution space, discover *terminal states*, i.e., states corresponding to a full program, and extract paths that lead to those states.

Clearly, the advantage of this reduction is that as execution space is smaller, the search problem becomes easier. Moreover, we can score each state based on many paths that lead to that node rather than based on a single path only.

Our approach is similar to the DPD algorithm (Pasupat and Liang, 2016), where CKY-style search is performed in denotation space, followed by search in a pruned space of programs for question answering. However, this search method was used without learning, and so the search was

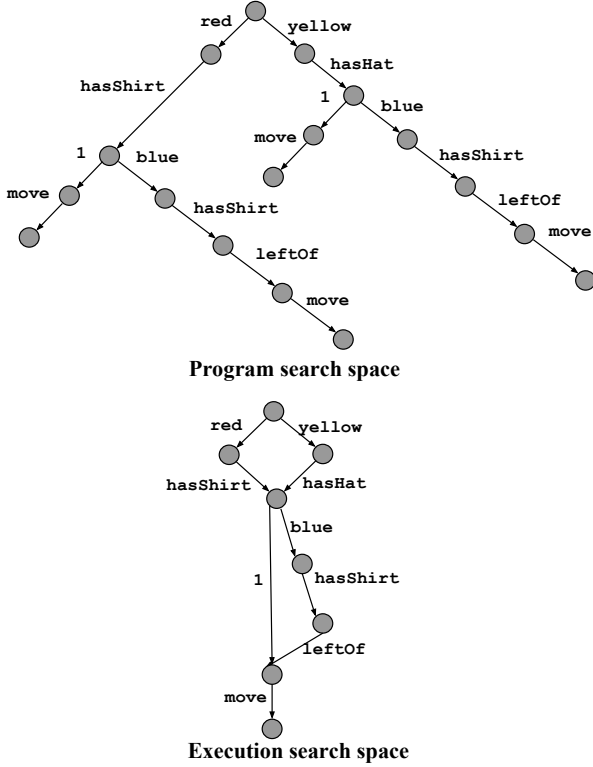


Figure 3: A set of commands represented in program space (top) and execution space (bottom). Since multiple prefixes have the same execution result (e.g., YELLOW HASHAT and RED HASSHIRT), execution space is more compact.

not guided by a trained model, which is a major part of our algorithm as we describe next.

4.2 Value-based Beam Search in Execution Space

We propose **Value-based Beam Search in eXecution space (VBSIX)**, a variant of beam search modified for searching in execution space.

Standard beam search is a breadth-first traversal of the program space tree, where a fixed number of vertices are kept in the beam at every level of the tree. The selection of vertices is done by scoring their corresponding prefixes $z_{1...t}$ according to $p_\theta(z_{1...t} | \mathbf{u}, c)$. The same traversal can be applied in execution space as well. However, since each vertex in execution space represents an execution result and not a particular prefix, we need to extend the scoring function to estimate the model probability for a vertex in execution space.

Let s be a vertex discovered in iteration t of the search. The state s will be scored according to $P_t[s]$, the probability to reach vertex s after t iterations³ according to the model p_θ . This probability

³We score paths in different iterations independently to

is the sum of probabilities of all prefixes of length t that reach s :

$$P_t[s] = \sum_{s'} P_{t-1}[s'] \cdot \left(\sum_{\{a: \delta(s', a) = s\}} \pi_\theta(a | s') \right).$$

VBSIX approximates $P_t[s]$ by performing this computation over the states in the beam B_{t-1} rather than all states, which can be done efficiently using dynamic programming (see Algorithm 1). This is a lower bound on the true model probability for this state, since there might be prefixes of length t that reach s that were not discovered.

Searching in execution space has significant advantages over standard beam search. First, since each vertex in execution space compactly represents multiple prefixes, a beam in VBSIX effectively holds more prefixes than standard beam search. Second, running search over a graph rather than a tree is less greedy, because the same vertex can surface back even if it fell out of the beam. Third, the scoring function of VBSIX is an aggregation over multiple paths in program space and therefore scores for states are more robust.

4.3 Value-based Ranker

Above, we scored a vertex s based on the sum of prefix probabilities leading to s . Alternatively, s can be scored based on the sum of suffix probabilities from s to correct terminal states, i.e., the expected reward of s :

$$V_\pi(s) = \sum_{\tau(s)} p_\theta(\tau(s) | s) \cdot R(\tau(s)),$$

where $\tau(s)$ are all possible trajectories starting from s and $R(\tau(s))$ is the reward observed when taking the trajectory $\tau(s)$ from s . Enumerating all trajectories $\tau(s)$ is intractable and so we will approximate $V_\pi(s)$ with a trained value network $V_\phi(s)$ parameterized by ϕ .

This value-based approach has several advantages: First, evaluating the probability of outgoing trajectories provides look-ahead that is missing from standard beam search. Second (and importantly), because we are focusing on search at training time, we can use the target denotation y as input to the value network and define it as $V_\phi(s, y)$. This lets the value network compare the denotation in the current state s to the target denotation y and get a better estimate for expected reward,

avoid bias towards shorter paths. A MDP state that appears in multiple iterations will get a different score in each iteration.

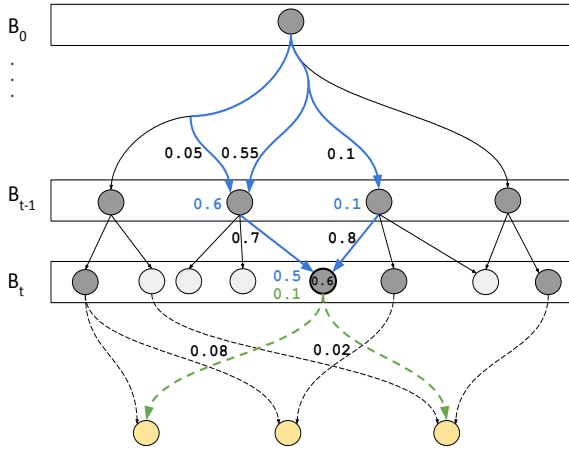


Figure 4: An illustration of scoring and pruning states in step t of VBSIX (see text for details). Discovered edges are in full edges, and undiscovered edges are dashed, correct terminal states are in yellow, states that are kept in the beam are in dark grey, actor scores are in blue, and critic scores in green.

especially in the later utterances of the sequence. This is similar in spirit to the actor-critic model for sequence-to-sequence proposed by (Bahdanau et al., 2017), where the full output sequence is observed, and to Suhr and Artzi (2018) who used the denotation to define a reward function.

Following Bahdanau et al. (2017) we call the probability $P_t[s]$ for a state s after t steps, *the actor score*, and the expected reward estimate $V_\phi(s, y)$ *the critic score*. We define the *actor-critic scoring function* as the sum of both scores. While conceptually the critic score is a natural scoring function in VBSIX, the two contributions are orthogonal: the critic score can be used in program space, and VBSIX can use the actor score only.

Figure 4 visualizes scoring and pruning the beam with the actor-critic scoring function in iteration t . Vertices in B_t are discovered by expanding vertices in B_{t-1} , and each vertex is ranked by the sum of the actor and critic scores. In the figure, the highlighted vertex has a score 0.6, which is a sum of the actor score (0.5) and the critic score (0.1). The actor score is the sum of its discovered incoming prefixes $((0.05 + 0.55) \cdot 0.7 + 0.01 \cdot 0.08 = 0.5)$ and the critic score is a value network estimation for the sum of probabilities for outgoing trajectories reaching correct terminal states $(0.02 + 0.08 = 0.1)$. Only the top- K states are kept in the beam ($K = 4$ in the figure).

Algorithm 1 summarizes our final proposed search algorithm at training time: VBSIX with an actor-critic scoring function. At a high level, the function PROGRAMSEARCH(\cdot) uses the VB-

Algorithm 1 Program Search with VBSIX

```

1: function PROGRAMSEARCH( $c, \mathbf{u}, y, \pi_\theta, V_\phi$ )
2:    $G, \mathcal{T} \leftarrow$  VBSIX( $c, \mathbf{u}, y, \pi_\theta, V_\phi$ )
3:    $\mathcal{Z} \leftarrow$  Find paths in  $G$  that lead to states in  $\mathcal{T}$  with
   beam search
4:   return  $\mathcal{Z}$ 
5: function VBSIX( $c, \mathbf{u}, y, \pi_\theta, V_\phi$ )
6:    $\mathcal{T} \leftarrow \emptyset, P \leftarrow \{\}$   $\triangleright$  init terminal states and DP chart
7:    $s_0 :=$  The empty program parsing state
8:    $B_0 \leftarrow \{s_0\}, G = (\{s_0\}, \emptyset)$   $\triangleright$  Init beam and graph
9:    $P_0[s_0] \leftarrow 1$   $\triangleright$  The probability of  $s_0$  is 1
10:  for  $t \in [1 \dots L]$  do
11:     $B_t \leftarrow \emptyset$ 
12:    for  $s \in B_{t-1}, a \in \mathcal{A}$  do
13:       $s' \leftarrow \delta(s, a)$ 
14:      Add edge  $(s, s')$  to  $G$  labeled with  $a$ 
15:      if  $s'$  is terminal then
16:         $\mathcal{T} \leftarrow \mathcal{T} \cup \{s'\}$ 
17:      else
18:         $P_t[s'] \leftarrow P_t[s'] + P_{t-1}[s] \cdot \pi_\theta(a|s)$ 
19:         $B_t \leftarrow B_t \cup \{s'\}$ 
20:      Sort  $B_t$  by AC-SCORER( $\cdot$ )
21:       $B_t \leftarrow$  Keep the top- $K$  states in  $B_t$ 
22:    Return  $G, \mathcal{T}$ 
23: function AC-SCORER( $s, P_t, V_\phi, y$ )
24:  Return  $P_t[s] + V_\phi(s, y)$ 

```

SIX procedure to construct a small search graph G and a set of terminal states \mathcal{T} . Then, standard beam search (in program space, with actor score) is applied on this small graph to extract a set of programs \mathcal{Z} (lines 2-4). Full details of programs' extraction from G are given in Appendix C. The programs \mathcal{Z} are used to update the models π_θ and V_ϕ (Section 5).

The VBSIX function receives as input a context c , an utterance sequence \mathbf{u} , a target denotation y , an actor model π_θ and a value network V_ϕ , and returns a graph G and a set of terminal states \mathcal{T} . VBSIX begins exploration from s_0 , the state of the empty program (lines 7-9). At every step t , the algorithm constructs the beam B_t , a set of states that can be reached from s_0 in t steps, P_t , a dynamic programming (DP) chart mapping each state to its actor score in iteration t , and the graph G (lines 10-21). P_t and B_t are updated for every newly discovered state (lines 18-19), and terminal states are added to \mathcal{T} (line 16). B_t is scored and pruned according to the sum of the actor score P_t and the value function V_ϕ (line 24). Since the value function and DP chart are used for efficient ranking, the asymptotic run-time complexity of VBSIX is the same as standard beam search ($\mathcal{O}(K \cdot |\mathcal{A}| \cdot L)$). The beam search in the path-extraction step (Line 3) can be done with a small beam size, since it operates over a small graph,

Algorithm 2 Actor-Critic Training

```
1: procedure TRAIN()
2:   Initialize  $\theta$  and  $\phi$  randomly
3:   while  $\pi_\theta$  not converged do
4:      $(x := (c, \mathbf{u}), y) \leftarrow$  select random example
5:      $\mathcal{Z} \leftarrow$  PROGRAMSSEARCH( $c, \mathbf{u}, y, \pi_\theta, V_\phi$ )
6:      $\mathcal{D}_v \leftarrow$  BUILDVALUEEXAMPLES( $\mathcal{Z}, c, y$ )
7:     Update  $\phi$  using  $\mathcal{D}_v$ , update  $\theta$  using  $(x, y)$ 
8:   function BUILDVALUEEXAMPLES( $\mathcal{Z}, c, \mathbf{u}, y$ )
9:     for  $z \in \mathcal{Z}$  do
10:    for  $t \in [1 \dots |z|]$  do
11:       $s \leftarrow \llbracket z_{1\dots t} \rrbracket_c^{e_x}$ 
12:       $L[s] \leftarrow L[s] + p_\theta(z_{t\dots|z}|c, \mathbf{u}) \cdot R(z)$ 
13:     $\mathcal{D}_v \leftarrow \{((s, y), L[s])\}_{s \in L}$ 
14:    Return  $\mathcal{D}_v$ 
```

and so its contribution to algorithm complexity is negligible.

5 Training

We train the model π_θ and value network V_ϕ jointly, where π_θ is trained using MML as described in Section 2, and the value network is trained as we explain next (Algorithm 2). Given a training example (c, \mathbf{u}, y) , we first generate a set of programs \mathcal{Z} with VBSIX. We then construct a set of training examples \mathcal{D}_v , where each example $((s, y), l)$ labels states encountered while generating programs $z \in \mathcal{Z}$ with the probability mass of correct programs suffixes that extend it, i.e., $l = \sum_{z_t} p_\theta(z_{t\dots|z}|c)$, where z_t ranges over all $z \in \mathcal{Z}$ and $t \in [1 \dots |z|]$. Finally, we train V_ϕ to maximize the objective:

$$\sum_{((s,y),l) \in \mathcal{D}_v} l \cdot \log V_\phi(s,y) + (1-l) \cdot (\log(1 - V_\phi(s,y)))$$

Similar to the estimation of $P_t[s]$, labeling examples for the value network is affected by beam-search errors: the labels are a lower bound for the true expected reward, since correct programs might fall off the beam. However, since search is guided by the model, those programs are likely to have low probability and their contribution to the true expected reward negligible. Moreover, estimates from the value network are based on training over multiple examples, while model probability estimates are based on a DP chart for one particular example. This makes the value network more robust to beam search errors.

Neural network architecture: We adapt the model proposed by Guu et al. (2017) for SCONE. The model receives the current utterance u^i and the program stack ψ , and returns a distribution

over the valid next tokens. Our value network receives the the same input, but also the next utterance u^{i+1} , the current world state w^i and the target world state y , and outputs a scalar. Appendix A provides a full description of the architecture.

6 Experiments

6.1 Experimental setup

We evaluate our method on the three domains of SCONE, evaluating with the standard accuracy metric, i.e., the proportion of test examples where the program generated by the model produced the correct denotation y . We train with VBSIX, and use standard beam search at test time to generate a set of programs and pick the one with highest model probability. Each test example contains 5 utterances, and similar to prior work we report the accuracy of each model on all 5 utterances as well as the first 3 utterances. We run each experiment 6 times with different random seeds and report the average accuracy and standard deviation.

In contrast to prior work on SCONE (Long et al., 2016; Guu et al., 2017; Suhr and Artzi, 2018), where models were trained on all sequences of 1 or 2 utterances, and thus were exposed during training to all gold intermediate states, we train from longer sequences keeping intermediate states latent. This leads to a harder search problem that was not addressed previously, but makes our results incomparable to previous results. In SCENE and TANGRAM, we used the first 4 and 5 utterances as examples. In ALCHEMY, we used the first utterance and the full 5 utterances.

Training details To warm-start the value network, we train for a few thousand steps, and only then start re-ranking with its predictions. Moreover, we gain efficiency by first returning K_0 (=128) states with the actor score only, and then re-ranking those with the actor-critic score and returning K (=32) states. Last, we use the value network only in the last two utterances of every example since we found it has less effect in earlier utterances where future uncertainty is large.

In all experiments training is performed with the Adam optimizer (Kingma and Ba, 2014). We used fixed GloVe vectors (Pennington et al., 2014) to embed utterance words, and all other parameters were initialized randomly.

Baselines We evaluate the following models:

	SCENE		ALCHEMY		TANGRAM	
	3 utt	5 utt	3 utt	5 utt	3 utt	5 utt
REINFORCE	0±(0.0)	0±(0.0)	0±(0.0)	0±(0.0)	0±(0.0)	0±(0.0)
MML	8.1±(2.4)	7.1±(1.2)	41.6±(22.9)	33.0±(20.0)	32.5±(20.7)	16.8±(14.1)
VBSIX	33.4±(26.8)	27.6±(20.8)	74.5±(1.1)	64.8±(1.5)	65.0±(0.8)	43.0±(1.3)

Table 1: Test accuracy and standard deviation of VBSIX compared to multiple baselines. We evaluate the same model over the first 3 and 5 utterances in each domain.

Search space	Value	SCENE		ALCHEMY		TANGRAM	
		3 utt	5 utt	3 utt	5 utt	3 utt	5 utt
Program	No	4.5±(0.6)	4.0±(1.4)	37.0±(26.5)	26.2±(24.0)	34.4±(18.3)	15.6±(12.8)
Execution	No	7.4±(10.4)	4.0±(5.8)	41.3±(28.6)	28.2±(23.27)	33.5±(15.5)	12.7±(10.4)
Program	Yes	10.4±(19.3)	7.2±(12.4)	75.2±(3.8)	69.7±(4.6)	65.7±(3.0)	39.5±(3.8)
Execution	Yes	30.6±(25.2)	22.5±(19.0)	81.9±(1.3)	75.2±(2.9)	68.6±(2.0)	44.2±(2.1)

Table 2: Validation accuracy when ablating the different components of VBSIX. The first line presents MML, the last line is VBSIX, and the intermediate lines examine execution space and value-based networks separately.

1. MML: Our main baseline, where search is done with beam search and training with MML. We use randomized beam-search, which adds ϵ -greedy exploration to beam search, which was proposed by Guu et al. (2017) and performed better.⁴
2. REINFORCE (Williams, 1992; Sutton et al., 1999): We followed the implementation of Guu et al. (2017), who perform variance reduction with a constant baseline and added ϵ -greedy exploration.
3. VBSIX: Our full model that ranks states with an actor-critic score and searches in execution space.

The full list of hyper-parameters such as beam size, learning rate, etc. are reported in appendix B.

6.2 Results

Table 1 reports test accuracy of VBSIX compared to the baselines. First, VBSIX outperforms all baselines in all cases. Similar to recent findings,⁵ REINFORCE is unable to find good programs to bootstrap from and training fails. MML performs much better, especially on ALCHEMY and TANGRAM, but is still almost 30 points lower than VBSIX on average.

On top of the improvement in accuracy, the standard deviation of VBSIX is lower than the other baselines across the 6 random seeds, showing the robustness of our model. One exception is the SCENE domain, where the language is more complex and absolute accuracies are lower. The performance of other baselines is quite low and consequently also the standard deviation.

⁴We did not include meritocratic updates (Guu et al., 2017), since it performed worse in initial experiments.

⁵<http://www.argmin.net/2018/02/20/reinforce/>

Ablations We perform ablation tests to examine the benefit of our two main technical contributions (a) execution space (b) value-based beam search. Table 2 presents the accuracy results on the validation set when each component is used separately, when both of them are used (VBSIX), and when none are used (beam-search). We find that both contributions are important for the final performance, as the full system achieves the highest accuracy across all domains. In SCENE, each component separately has only a slight advantage over beam-search, and therefore both components are required to achieve significant improvement. However, in ALCHEMY and TANGRAM most of the gain is due to the value network.

In addition to validation accuracy, we can also directly measure *hit accuracy* at training time, i.e., the proportion of training examples where the beam produced by the search algorithm contains a program with the correct denotation. This measures the effectiveness of search at training time directly. In Figure 5, we show the train hit accuracy in each training step, averaged across the 6 random seeds. The graphs illustrate the performance of each search algorithm in every domain, and the improvement of the model during training. We observe that validation accuracy results are well-correlated with the improvement in hit accuracy, showing that the better performance can be mostly attributed to the search algorithm.

6.3 Analysis

We analyze the ability of the value network to predict expected reward. The reward of a state depends on two properties, (a) *connectivity*: whether there is a trajectory from this state to a correct terminal state, and (b) *model likelihood*: the proba-

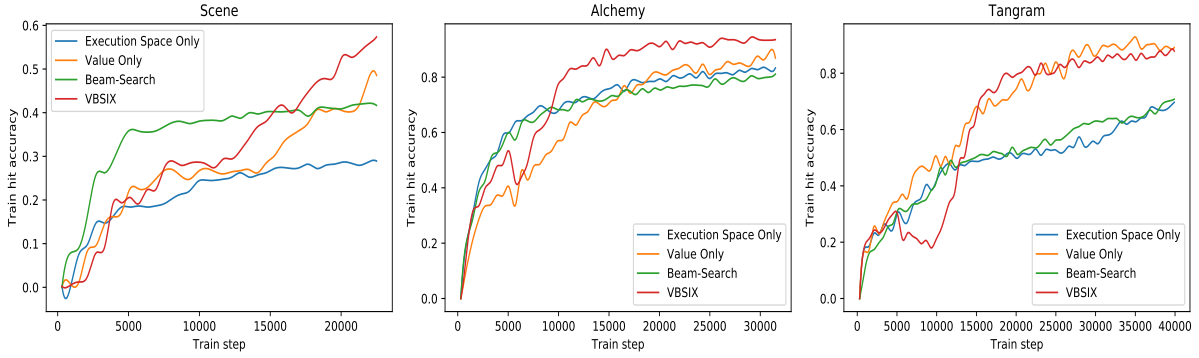


Figure 5: Training hit accuracy on examples with 5 utterances, comparing VBSIX to baselines with ablated components. The results are averaged over 6 runs with different random seeds.

bility the model assigns to those trajectories. We collected a random set of 120 states in the SCENE domain from, where the real expected reward was very high (> 0.7), or very low ($= 0.0$) and the value network predicted well (less than 0.2 deviation) or poorly (more than 0.5 deviation). For ease of analysis we only look at states from the final utterance.

To analyze connectivity, we looked at states that cannot reach a correct terminal state with a single action (since states in the last utterance can perform one action only, the expected reward is 0). Those are states where either their current and target world differ in too many ways, or the stack content is not relevant to the differences between the worlds. We find that when there are many differences between the current and target world, the value network correctly estimates low expected reward in 87.0% of the cases. However, when there is just one mismatch between the current and target world, the value network tends to ignore it and erroneously predicts high reward in 78.9% of the cases.

To analyze whether the value network can predict the success of the trained policy, we consider states from which there is an action that leads to the target world. While it is challenging to fully interpret the value network, we notice that the network predicts a value that is > 0.5 in 86.1% of the cases where the number of people in the world is no more than 2, and a value that is < 0.5 in 82.1% of the cases where the number of people in the world is more than 2. This indicates that the value network believes more complex worlds, involving many people, are harder for the policy.

7 Related Work

Training from denotations has been extensively investigated in both question answering (Clarke et al., 2010; Liang et al., 2011; Berant et al., 2013; Kwiatkowski et al., 2013; Pasupat and Liang, 2015) and instruction mapping (Branavan et al., 2009; Artzi and Zettlemoyer, 2013; Bisk et al., 2016), with a recent emphasis on neural encoder-decoder models (Guu et al., 2017; Cheng et al., 2017; Neelakantan et al., 2016; Krishnamurthy et al., 2017; Liang et al., 2017, 2018; Goldman et al., 2018). Understanding instructions has been studied with the SAIL corpus (MacMahon et al., 2006; Chen and Mooney, 2011; Andreas and Klein, 2015; Mei et al., 2016) and recently with other environments, focusing on single sentence instructions (Janner et al., 2018; Misra et al., 2018; Anderson et al., 2018; Tan and Bansal, 2018).

Tackling the limitations of beam search has been investigated recently by proposing objectives suitable for beam search (Wiseman and Rush, 2016), by using continuous relaxation that afford differentiability (Goyal et al., 2018), and by developing specialized stopping criteria (Yang et al., 2018).

Similar to our work, Bahdanau et al. (2017) and Suhr and Artzi (2018) proposed ways to evaluate the predictions at intermediate steps from a sparse reward signal. Bahdanau et al. (2017) used a critic network to estimate the expected BLEU score in translation, while Suhr and Artzi (2018) used the edit-distance between the current world state and the goal world state in the SCONE task. However, in those works stronger supervision was assumed: Bahdanau et al. (2017) utilized the gold sequences, and Suhr and Artzi (2018) used intermediate worlds states. Moreover, in their work in-

intermediate evaluations were used to compute the gradient updates, rather than for guiding search.

Guiding search with both a policy and value networks was done in recent work on Monte-Carlo Tree Search (MCTS) for sparse-reward tasks (Silver et al., 2017; T. A. and Barber, 2017; Shen et al., 2018). In MCTS, the value network evaluations are refined with backup updates in order to gain an advantage over the policy scores. However, in our implementation we gain this advantage by simply feeding the denotation to the value network. We also note that the additive interpolation between an actor and a critic are reminiscent of A^* algorithm where states are scored by adding past cost and an admissible heuristic for future cost (Klein and Manning, 2003; Pauls and Klein, 2009; lee et al., 2016).

8 Conclusions

In this work, we propose a new training algorithm for mapping instruction to programs given denotation supervision only. Our algorithm exploits the denotation at training time to train a critic network that is used to rank search states on the beam, and performs search in a compact space of execution results rather than in the space of programs. We evaluate our algorithm on three different domains from the SCONE dataset, and find that it dramatically improves performance compared to strong baselines across all domains.

References

- P. Anderson, Q. Wu, D. Teney, J. Bruce, M. Johnson, N. Sünderhauf, I. Reid, S. Gould, and A. van den Hengel. 2018. Vision-and-language navigation: Interpreting visually-grounded navigation instructions in real environments. In *Computer Vision and Pattern Recognition (CVPR)*.
- J. Andreas and D. Klein. 2015. Alignment-based compositional semantics for instruction following. In *Empirical Methods in Natural Language Processing (EMNLP)*.
- Y. Artzi and L. Zettlemoyer. 2013. Weakly supervised learning of semantic parsers for mapping instructions to actions. *Transactions of the Association for Computational Linguistics (TACL)*, 1:49–62.
- D. Bahdanau, P. Brakel, K. Xu, A. Goyal, R. Lowe, J. Pineau, A. Courville, and Y. Bengio. 2017. An actor-critic algorithm for sequence prediction. In *International Conference on Learning Representations (ICLR)*.
- J. Berant, A. Chou, R. Frostig, and P. Liang. 2013. Semantic parsing on Freebase from question-answer pairs. In *Empirical Methods in Natural Language Processing (EMNLP)*.
- Y. Bisk, D. Yuret, and D. Marcu. 2016. Natural language communication with robots. In *North American Association for Computational Linguistics (NAACL)*.
- S. Branavan, H. Chen, L. S. Zettlemoyer, and R. Barzilay. 2009. Reinforcement learning for mapping instructions to actions. In *Association for Computational Linguistics and International Joint Conference on Natural Language Processing (ACL-IJCNLP)*, pages 82–90.
- D. L. Chen and R. J. Mooney. 2011. Learning to interpret natural language navigation instructions from observations. In *Association for the Advancement of Artificial Intelligence (AAAI)*, pages 859–865.
- J. Cheng, S. Reddy, V. Saraswat, and M. Lapata. 2017. Learning structured natural language representations for semantic parsing. In *Association for Computational Linguistics (ACL)*.
- J. Clarke, D. Goldwasser, M. Chang, and D. Roth. 2010. Driving semantic parsing from the world’s response. In *Computational Natural Language Learning (CoNLL)*, pages 18–27.
- O. Goldman, V. Laticinnik, U. Naveh, A. Globerson, and J. Berant. 2018. Weakly-supervised semantic parsing with abstract examples. In *Association for Computational Linguistics (ACL)*.
- K. Goyal, G. Neubig, C. Dyer, and T. Berg-Kirkpatrick. 2018. A continuous relaxation of beam search for end-to-end training of neural sequence models. In *Association for the Advancement of Artificial Intelligence (AAAI)*.
- K. Guu, P. Pasupat, E. Z. Liu, and P. Liang. 2017. From language to programs: Bridging reinforcement learning and maximum marginal likelihood. In *Association for Computational Linguistics (ACL)*.
- S. Hochreiter and J. Schmidhuber. 1997. Long short-term memory. *Neural Computation*, 9(8):1735–1780.
- M. Janner, K. Narasimhan, and R. Barzilay. 2018. Representation learning for grounded spatial reasoning. *Transactions of the Association for Computational Linguistics (TACL)*, 6.
- D. Kingma and J. Ba. 2014. Adam: A method for stochastic optimization. *arXiv preprint arXiv:1412.6980*.
- D. Klein and C. Manning. 2003. A^* parsing: Fast exact viterbi parse selection. In *Human Language Technology and North American Association for Computational Linguistics (HLT/NAACL)*.

- J. Krishnamurthy, P. Dasigi, and M. Gardner. 2017. Neural semantic parsing with type constraints for semi-structured tables. In *Empirical Methods in Natural Language Processing (EMNLP)*.
- J. Krishnamurthy and T. Mitchell. 2012. Weakly supervised training of semantic parsers. In *Empirical Methods in Natural Language Processing and Computational Natural Language Learning (EMNLP/CoNLL)*, pages 754–765.
- T. Kwiatkowski, E. Choi, Y. Artzi, and L. Zettlemoyer. 2013. Scaling semantic parsers with on-the-fly ontology matching. In *Empirical Methods in Natural Language Processing (EMNLP)*.
- K. Lee, M. Lewis, and L. Zettlemoyer. 2016. Global neural CCG parsing with optimality guarantees. In *Empirical Methods in Natural Language Processing (EMNLP)*.
- C. Liang, J. Berant, Q. Le, and K. D. F. N. Lao. 2017. Neural symbolic machines: Learning semantic parsers on Freebase with weak supervision. In *Association for Computational Linguistics (ACL)*.
- C. Liang, M. Norouzi, J. Berant, Q. Le, and N. Lao. 2018. Memory augmented policy optimization for program synthesis with generalization. In *Advances in Neural Information Processing Systems (NIPS)*.
- P. Liang, M. I. Jordan, and D. Klein. 2011. Learning dependency-based compositional semantics. In *Association for Computational Linguistics (ACL)*, pages 590–599.
- R. Long, P. Pasupat, and P. Liang. 2016. Simpler context-dependent logical forms via model projections. In *Association for Computational Linguistics (ACL)*.
- M. MacMahon, B. Stankiewicz, and B. Kuipers. 2006. Walk the talk: Connecting language, knowledge, and action in route instructions. In *National Conference on Artificial Intelligence*.
- H. Mei, M. Bansal, and M. R. Walter. 2016. Listen, attend, and walk: Neural mapping of navigational instructions to action sequences. In *Association for the Advancement of Artificial Intelligence (AAAI)*.
- D. Misra, A. Bennett, V. Blukis, E. Niklasson, M. Shatkhin, and A. Yoav. 2018. Mapping instructions to actions in 3D environments with visual goal prediction. In *Empirical Methods in Natural Language Processing (EMNLP)*.
- A. Neelakantan, Q. V. Le, and I. Sutskever. 2016. Neural programmer: Inducing latent programs with gradient descent. In *International Conference on Learning Representations (ICLR)*.
- P. Pasupat and P. Liang. 2015. Compositional semantic parsing on semi-structured tables. In *Association for Computational Linguistics (ACL)*.
- P. Pasupat and P. Liang. 2016. Inferring logical forms from denotations. In *Association for Computational Linguistics (ACL)*.
- A. Pauls and D. Klein. 2009. K-best A* parsing. In *Association for Computational Linguistics (ACL)*, pages 958–966.
- J. Pennington, R. Socher, and C. D. Manning. 2014. GloVe: Global vectors for word representation. In *Empirical Methods in Natural Language Processing (EMNLP)*, pages 1532–1543.
- Y. Shen, J. Chen, P. Huang, Y. Guo, and J. Gao. 2018. Reinforcewalk: Learning to walk in graph with monte carlo tree search. In *International Conference on Learning Representations (ICLR)*.
- D. Silver, J. Schrittwieser, K. Simonyan, I. Antonoglou, A. Huang, A. Guez, T. Hubert, L., M. Lai, A. Bolton, et al. 2017. Mastering the game of go without human knowledge. *Nature*, 550(7676):354–359.
- A. Suhr and Y. Artzi. 2018. Situated mapping of sequential instructions to actions with single-step reward observation. In *Association for Computational Linguistics (ACL)*.
- I. Sutskever, O. Vinyals, and Q. V. Le. 2014. Sequence to sequence learning with neural networks. In *Advances in Neural Information Processing Systems (NIPS)*, pages 3104–3112.
- R. Sutton, D. McAllester, S. Singh, and Y. Mansour. 1999. Policy gradient methods for reinforcement learning with function approximation. In *Advances in Neural Information Processing Systems (NIPS)*.
- Z. Tian T. A. and D. Barber. 2017. *Thinking Fast and Slow with Deep Learning and Tree Search*. Advances in Neural Information Processing Systems 30.
- H. Tan and M. Bansal. 2018. Source-target inference models for spatial instruction understanding. In *Association for the Advancement of Artificial Intelligence (AAAI)*.
- A. Vogel and D. Jurafsky. 2010. Learning to follow navigational directions. In *Association for Computational Linguistics (ACL)*, pages 806–814.
- R. J. Williams. 1992. Simple statistical gradient-following algorithms for connectionist reinforcement learning. *Machine learning*, 8(3):229–256.
- S. Wiseman and A. M. Rush. 2016. Sequence-to-sequence learning as beam-search optimization. In *Empirical Methods in Natural Language Processing (EMNLP)*.
- Y. Yang, L. Huang, and M. Ma. 2018. Breaking the beam search curse: A study of (re-) scoring methods and stopping criteria for neural machine translation. In *Empirical Methods in Natural Language Processing (EMNLP)*.

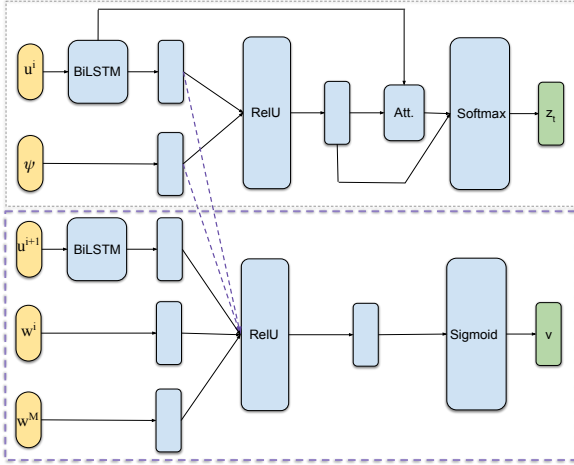


Figure 6: The model proposed by Guu et al. (2017) (top), and our value network (bottom).

A Neural Network Architecture

We adopt the model $\pi_\theta(\cdot)$ proposed by Guu et al. (2017). The model receives the current utterance u^i and the program stack ψ . A bidirectional LSTM (Hochreiter and Schmidhuber, 1997) is used to embed u_i , while ψ is embedded by concatenating the embedding of stack elements. The embedded input is then fed to a feed-forward network with attention over the LSTM hidden states, followed by a softmax layer that predicts a program token. Our value network $V_\phi(\cdot)$ shares the input layer of $\pi_\theta(\cdot)$. In addition, it receives the next utterance u^{i+1} , the current world state w^i and the target world state w^M . The utterance u^{i+1} is embedded with an additional BiLSTM, and world states are embedded by concatenating embeddings of SCONE elements. The inputs are concatenated and fed to a feed-forward network, followed by a sigmoid layer that outputs a scalar.

B Hyper-parameters

Table 3 contains the hyper-parameter setting for each experiment. Hyper-parameters of REINFORCE and MML were taken from Guu et al. (2017). In all experiments learning rate was 0.001 and mini-batch size was 8. We explicitly define the following hyper-parameters which are not self-explanatory:

1. *Sample size*: Number of samples drawn from p_θ in REINFORCE
2. *Baseline*: A constant subtracted from the reward for variance reduction.
3. *Execution beam size*: K in Algorithm 1.
4. *Program bea size*: Size of beam in line 3 of

Algorithm 1.

5. *Value ranking start step*: Step when we start ranking states using the critic score.

6. *Value re-rank size*: Size of beam K_0 returned by the actor score before re-ranking with the actor-critic score.

C Programs' Extraction

We denote G to be the search-graph found in the execution-search. The paths in G that lead to terminal states represent the discovered programs. A program's correctness is determined by the correctness of its terminal state, i.e whether the state's world matches the target world.

We extract correct and incorrect programs separately. Correct programs are built with standard beam search (guided by our model π_θ) over prefixes in G , that their states are connected to correct terminal states. The search is therefore restricted to the space of the correct found programs. Incorrect programs are built by selecting, for each incorrect terminal state in G , a single path that leads to it.

System	SCENE	ALCHEMY	TANGRAM
REINFORCE	Sample size = 32 $\epsilon = 0.2$ Baseline = 10^{-5}	Sample size = 32 $\epsilon = 0.2$ Baseline = 10^{-2}	Sample size = 32 $\epsilon = 0.2$ Baseline = 10^{-3}
MML	Beam size = 32 $\epsilon = 0.15$	Beam size = 32 $\epsilon = 0.15$	Beam size = 32 $\epsilon = 0.15$
VBSiX	Execution beam size = 32 Program beam size = 8 $\epsilon = 0.15$ Value ranking start step = $5k$ Value re-rank size = 128	Execution beam size = 32 Program beam = 8 $\epsilon = 0.15$ Value ranking start step = $5k$ Value re-rank size = 128	Execution beam size = 32 Program beam size = 8 $\epsilon = 0.15$ Value ranking start step = $10k$ Value re-rank size = 128

Table 3: Hyper-parameter settings.